Cell Transplantation, Vol. 21, pp. 493–503, 2013

0963-6897/13 $90.00 + .00
DOI: http://dx.doi.org/10.3727/096368912X652977
E-ISSN 1555-3892
www.cognizantcommunication.com

In Situ Electrostimulation Drives a Regenerative Shift in the Zone of Infarcted Myocardium

Cristiano Spadaccio,* Alberto Rainer,† Federico De Marco,‡ Mario Lusini,* Paolo Gallo,§ Pietro Sedati,¶ Andrea Onetti Muda,# Stefano De Porcellinis,** Chiara Gregorj,†† Giuseppe Avvisati,†† Marcella Trombetta,† Massimo Chello,* Elvio Covino,* David A. Bull,‡‡ Amit N. Patel,‡‡ and Jorge A. Genovese*‡‡

*Center for Integrated Research, Department of Cardiovascular Science, Unit of Cardiac Surgery, Università Campus Bio-Medico di Roma, Rome, Italy
†Center for Integrated Research, Laboratory of Tissue Engineering, Università Campus Bio-Medico di Roma, Rome, Italy
‡Laboratory of Virology, Regina Elena Institute for Cancer Research, Rome, Italy
§Center for Integrated Research, Department of Cardiovascular Science, Unit of Cardiology, Università Campus Bio-Medico di Roma, Rome, Italy
¶Center for Integrated Research, Unit of Image Diagnostics, Università Campus Bio-Medico di Roma, Rome, Italy
#Center for Integrated Research, Department of Pathology, Università Campus Bio-Medico di Roma, Rome, Italy
**Biomatica Srl, Rome, Italy
††Center for Integrated Research, Department of Hematology, Università Campus Bio-Medico di Roma, Rome, Italy
‡‡Division of Cardiothoracic Surgery, Department of Surgery, University of Utah, Salt Lake City, UT, USA

Electrostimulation represents a well-known trophic factor for different tissues. In vitro electrostimulation of non-stem and stem cells induces myogenic predifferentiation and may be a powerful tool to generate cells with the capacity to respond to local areas of injury. We evaluated the effects of in vivo electrostimulation on infarcted myocardium using a miniaturized multiparameter implantable stimulator in rats. Parameters of electrostimulation were organized to avoid a direct driving or pacing of native heart rhythm. Electrical stimuli were delivered for 14 days across the scar site. In situ electrostimulation used as a cell-free, cytokine-free stimulation system, improved myocardial function, and increased angiogenesis through endothelial progenitor cell migration and production of vascular endothelial growth factor (VEGF). In situ electrostimulation represents a novel means to stimulate repair of the heart and other organs, as well as to precondition tissues for treatment with cell-based therapies.

Key words: Stem cells; Myocardium; Infarct; Electrostimulation (ES)

INTRODUCTION

Electrostimulation (ES) represents a well-known trophic factor for different tissues. In a multicellular organism, the function and fate of cells are tightly regulated and respond to environmental factors and intercellular signals (11). Neurodegenerative diseases affecting primary motoneurons are often associated with loss of muscle mass, suggesting that trophic factors and electrical stimuli play a pivotal role in the life cycle and function of muscle. It has been shown that the compensation, by controlled electrical stimulation, for the lack of electrical stimuli can increase muscle mass, leading to clinical improvement and quality of life (19). Although the mechanisms underlying the effect of electrical stimulation remain unclear, a considerable body of evidence has accumulated which points to the induction of cellular hypertrophy, regeneration (1,2,5,6), and inhibition of apoptosis (16,21,23,30,33). One group of researchers has reported that latissimus dorsi muscle flaps, preconditioned by long-term pacing for subsequent use in cardioplasty, undergo anatomopathological differentiation (3). Additionally, studies on biventricular pacing in sheep treated with intramyocardial injection of

Received April 14, 2011; final acceptance March 30, 2012. Onlne prepub date: July 10, 2012.
Address correspondence to Jorge A. Genovese at his current address: School of Medicine, Maimonides University, Hidalgo 775 6to Piso, (C1405BCK) Ciudad Autonoma de Bueneos Aires, Argentina. Tel: +541149051101/1113, ext. 1234;
E-mail: genovese.jorge@maimonides.edu

autologous myoblasts demonstrated enhanced production of myosin following electrostimulation (29).

In our prior studies, we hypothesized that stimulating a cardiac microenvironment by mimicking in vitro electrophysiological conditions and parameters of normal heart rhythm would promote differentiation toward cardiomyocyte phenotype. This ES-induced cardiac precommitment would use a cytokine-free culture system, thus avoiding potentially harmful demethylating agents or growth factors, which are limitations to the clinical application of cell therapy.

We tested this system on both non-stem and stem cells: (1) fibroblasts, which regulate cardiac extracellular matrix and represent the most abundant cell population in the region of a myocardial infarction, and (2) human mesenchymal stem cells, widely known for their rapid harvesting, amenable culturing properties and high plasticity (7,8). Predifferentiation resulted in several morphological changes, including multinucleated cells formation and cytoskeleton rearrangement. The expression of cardiac proteins related to cell contraction and intercellular communication appeared early. Myocardiocyte predifferentiation of stem and non-stem cells appears to be a potentially powerful tool to obtain cells with oriented evolutive capacity able to answer to signals in the local environment. These cells exhibit phenotypic and metabolic changes that facilitate their homing, adaptation, survival, replication, function, and resultant therapeutic effect (7,8).

The potential to induce a reorganization of the cell biosynthesis apparatus after a short period of electrostimulation led us to investigate mechanisms related to membrane modifications. In particular, ion channels aperture timing may be affected by ES, leading to transient changes in intracellular pH and nuclear transcriptional enzyme activation (8).

Interestingly, this system of predifferentiation was not a phenotype-restricted phenomenon but could be applied to both embryonic and adult non-stem and stem cell lines (7,8). We further investigated potential mechanisms underlying the effect of ES related to growth factors and molecular pathways. We performed a microarray on electrostimulated (ES) cells and a proteomic analysis on both ES cells and culture supernatants, and we isolated an important member of the transforming growth factor (TGF)-β superfamily, follistatin, as a potential candidate responsible for this phenomenon in stem cells (9).

Given these findings obtained with in vitro ES of fibroblast, we sought to reproduce our findings in vivo using an animal model of myocardial infarction by applying ES to scar fibroblasts in situ.

The role of ES in inducing angiogenesis, cell proliferation, and inhibition of apoptosis is widely known. Therefore, we also sought to determine whether ES induces angiogenesis and endothelial progenitor cell mobilization in an in vivo model of myocardial infarction. Specifically, we used a miniaturized multiparameter implantable stimulator to induce ES of the region surrounding a myocardial infarction. Parameters of ES were organized to avoid a direct driving or pacing of native heart rhythm. In this way, we could evaluate the global effects of the application of a variable electric field, which does not interfere with endogenous heart activity, at the site of an experimental myocardial infarction, to determine the effects of ES on cardiac function and to help to elucidate the mechanisms involved.

MATERIALS AND METHODS

General Overview

Female Wistar rats (16 weeks old, weighing 250–300 g, Charles River Laboratory) were used in the study. A total of 24 animals were divided in two groups. One group (treatment group) underwent nonpacing electrical stimulation by a previously described electrostimulator (25) for 2 weeks following induction of a myocardial infarction by ligation of the left anterior descending coronary artery. In the control group, electrodes were implanted but not activated following induction of the myocardial infarction. All procedures, care, and handling of the animals were reviewed and approved by the Institutional Animal Care and Use Committee of the Regina Elena Institute.

Operative Procedures

Anesthesia. Rats were anesthetized during the surgical procedure with 1.0–1.5% isoflurane (Abbott Laboratories, North Chicago, IL, USA) in 100% oxygen for induction and maintenance of anesthesia. Rats were endotracheally intubated and mechanically ventilated with a small animal respirator at a rate of 60–70 breaths per minute (Harvard Apparatus, Holliston, MA). Tidal volume was set to 2 ml/100 g of body weight. Rats were placed on a warming pad (37°C) in the supine position. The hair on the anterior and lateral chest wall was trimmed with an electric clipper. The skin leads of an electrocardiographic apparatus (Biomatica, Italy) were attached on both fore limbs and on the left hind limb, and the electrocardiogram was monitored. Before skin incision, one dose of cefuroxime (100 mg/kg) was administered intramuscularly for prophylaxis against surgical infection.

Myocardial Infarction Protocol. Surgery was performed using aseptic techniques with sterile instruments. The skin of the anterior chest wall was aseptically prepped with a povidone–iodine solution. The chest was opened at the fourth intercostal space, and the left anterior descending coronary artery was identified. Myocardial infarction was induced with ligation of the left anterior descending coronary artery 2 mm from the tip of the normally positioned left auricle as previously described (22).

Electrostimulation. Electrostimulator devices (manufactured and commercially available at the University of Liverpool, UK) were implanted accordingly to manufacturer's instructions with the electrodes placed in the formed myocardial scar and the power supply in the abdominal cavity. Devices delivered a 3-V pulse at a rate of 10 Hz (25). Electrocardiographic recordings during pacing confirmed a nondriving activity on heart rhythm of the electrical stimuli delivered. Electrostimulators had an internal light-based switch to enable/disable pacemaker functioning using a conventional flash illuminator.

Wound Closure and Recovery. Closure of the chest was performed as follows: a 6–0 suture (1 of 2) used to retract the upper rib during surgery was passed under the lower rib, taking care to avoid vital structures, and taking only the intercostal muscles. This was tied to approximate the ribs. The muscle layer was reformed using semi-interrupted 5–0 sutures to form a complete seal. The skin was closed with semi-interrupted 5–0 sutures. A dab of povidone–iodine solution was placed on the suture line. After closure of the chest and thorax evacuation, the animals were allowed to recover on a warming pad. When responsive to stimuli and able to maintain an upright posture, rats were returned to the home cage and analgesia initiated. Buprenorphine (0.5 mg/kg) analgesic and cefuroxime (100 mg/kg) antibiotic were administered intramuscularly twice a day for 3 days after surgery.

Functional Assessment

Angio-Computed Tomography. AngioCT (Siemens AG, Erlangen, Germany) was performed on treatment and control groups to assess the efficacy of myocardial infarction induction. An additional group of healthy animals was added for comparison. Rats were anesthetized with midazolam at a dose of 2 mg/kg intramuscular. Electrocardiography (ECG) gating was achieved, iodated contrast medium injected in the tail vein, and cardiac computed tomography (CT) scans were obtained and reformatted in 3D using maximum intensity projection (MIP) and volume rendering algorithms. Left ventricular end-diastolic (LVEDD) and end-systolic (LVESD) diameters were measured by two independent blinded observers.

Echocardiography. Functional assessment was achieved by echocardiography, performed by a blinded investigator on control and treatment groups using a Sequoia C256 system (Acuson, Mountain View, CA, USA) equipped with a 13-MHz linear array transducer (15L8). Rats were anesthetized with isoflurane gas (3% isoflurane for 1 min induction and 1.25–1.5% isoflurane for maintenance) and restrained in the supine position. Echocardiography was performed 15 min after isoflurane induction on each rat. Although isoflurane gas may have a slight variable cardiodepressant effect, a recent report indicates that echocardiographic assessment of cardiac function in rodents anesthetized with isoflurane gas was comparable to that in anaesthetized conscious rodents (32). End-diastolic (EDV) and end-systolic (ESV) volumes were measured, and ejection fraction (EF) was calculated as follows:

$$\mathrm{EF}\,(\%) = \frac{\mathrm{EDV} - \mathrm{ESV}}{\mathrm{EDV}} \times 100$$

Histology and Structural Evaluation

Rats were humanely sacrificed and their hearts harvested, frozen in 2-methylbutane precooled in liquid nitrogen, and serially cryosectioned (from the apex to the base of each heart) into sections 5–10 μm thick. Masson's Modified Trichrome Stain Kit (IMEB, San Marcos, CA) and hematoxylin/eosin were used to stain the infarct scar according to the manufacturer's instructions. Immunohistochemistry for vascular endothelial growth factor (VEGF) and cluster of differentiation 34 (CD34) was performed as previously described (7). Briefly, sections were fixed and incubated with mouse anti-rat VEGF (at a dilution of 1:100) and CD34 (1:100) primary antibodies (Sigma, Milwaukee, MA) at 37°C. Horseradish peroxidise-conjugated secondary antibodies and 3-3′-diaminobenzidine were used to detect antibody binding. Slides were viewed under a light microscope (Nikon F100) by blinded observers and positive staining evaluated by Image-Pro Plus imaging software (Media Cybernetics, Inc., Bethesda, MD).

RT-PCR

Total cellular RNA was isolated using RNeasy mini kit (Qiagen, Inc., Valencia, CA) according to the manufacturer's protocol. To eliminate DNA contamination, samples were treated with 2.0 U of DNase I (Invitrogen, Carlsbad, CA) at 37°C for 15 min followed by inactivation with the addition of EDTA 2 mM at 65°C for 10 min according to the manufacturer's instructions. Reverse transcriptase-polymerase chain reaction (RT-PCR) was performed to detect the expression of atrial natriuretic peptide (ANP), VEGF, and β-actin, as housekeeping gene, using specific primers (Table 1) and Superscript One-Step RT-PCR (Invitrogen) for cDNA synthesis. PCR amplification was carried out for a total of 35 cycles using SYBR-Green PCR master mix (Invitrogen) in a total volume of 30 μl, according to the protocol and thermal profile reported in Table 1. Amplification products were identified by size on a 2% agarose gel.

Endothelial Progenitor Cells (EPCs) Count and Flow Cytometric Analysis

EPC count was performed by flow cytometry as previously described (27) on a fluorescence-activated cell

Table 1. Primers for Gene Expression

Gene	Primer Sequence	Protocol
ANP	Up: 5′- ATG GGC TCC TTC TCC ATC ACC -3′	94°C 30 s, 58°C 30 s, 72°C 1 min
	Down: 5′- GTA CCG GAA GCT GTT GCA GCC -3′	35 cycles
VEGF	Up: 5′- CCAGCACATAGGAGAGATGAGCTTC -3′	94°C 20 s, 55°C 30 s, 72°C 1 min
	Down: 5′- GGTGTGGTGGTGACATGGTTAATC -3′	35 cycles
β-Actin	Up: 5′- GCCATGTACGTAGCCATCCA -3′	94°C 20 s, 55°C 30 s, 72°C 1 min
	Down: 5′- GAACCGCTCATTGCCGATAG -3′	35 cycles

ANP, atrial natriuretic peptide; VEGF, vascular endothelial growth factor.

sorting (FACS) Diva flow cytometer (BD Biosciences, Franklin Lakes, NJ). Briefly, a volume of 100 µl of peripheral blood was incubated for 15 min with 2 ml of 1× ammonium chloride lysis buffer (BD Biosciences). Cells were then incubated for 15 min in the dark with monoclonal antibodies against rat CD34 and CD45. Isotype-identical antibodies served as controls (BD Biosciences). After incubation, cells were washed with 2 ml washing solution (BD Biosciences), centrifuged at 500 × *g* for 5 min, and resuspended in 500 µl washing solution (BD Biosciences). Before each analysis, 7-amino-actinomycin-D was added as a viability stain. Each analysis included 100,000 events within the lymphocyte gate. The $CD34^+$ population was expressed as the number of circulating cells per 100,000 lymphocytes (EPCs/lymphocytes) and, after adjustment for the number of leukocytes in peripheral blood and the fraction of lymphocytes/leukocytes, as the percentage of EPCs per 100 µl blood (EPCs/blood).

Statistical Analysis

All the experiments were performed in triplicate. Data are reported as the mean ± standard deviation. Data were processed using SPSS (Statistical Package for Social Sciences) release 13.0 for Windows (IBM, Somers, NY). One-way ANOVA was performed to compare groups subjected to different treatments, followed by multiple pairwise comparison procedure (Tukey test). Significance was at the 0.05 level.

RESULTS

The effects of in vivo ES were studied in a rat model of myocardial infarction. Electrical stimuli were delivered for 14 days across the scar site by a miniaturized device (Fig. 1). Evaluation of the effects of in situ ES in terms of cardiac function, histopathology, and angiogenesis was performed.

Functional Assessment

AngioCT scans showed defined areas of hypoperfusion in the region of the myocardial infarction (Fig. 2). Infarction resulted in an increased ventricular diameter compared to preoperative status, but no statistically significant difference was found between treatment and control groups (Fig. 2D). Echocardiography showed a significantly improved ejection fraction (EF) in the ES group compared to the control group (Fig. 3).

Histological Assessment

Masson's trichrome and H&E stainings were used to define and characterize, respectively, the infracted area (Fig. 4). Within the infarcted area, the ES group showed the presence of an eosinophilic, elongated, spindle-shaped cell population oriented in a parallel fashion in the proximity to the site of the electrode implant. These cells had an eccentric nucleus and a fine granularity in the cytoplasm (Fig. 5). These morphological findings were comparable to the cytologic characteristics present in our previously published in vitro experiments of ES with both light microscopy and ultrastructural analysis with electron microscopy. Along with these findings, numerous vascular structures could be identified in the treatment group (Fig. 5D). Immunohistology revealed the increased presence of endothelial progenitor cells ($CD34^+$) in the ES group (Fig. 6). Additionally, a higher level of VEGF was found in the group treated with electrical stimuli. The findings of increased numbers of both $CD34^+$ cells and levels of VEGF were subsequently confirmed by RT-PCR (Fig. 7) and flow cytometry (Fig. 8).

RT-PCR

RT-PCR for VEGF showed a significantly higher expression of VEGF in the treatment group (Fig. 7C, E). Conversely, ANP expression was reduced in the treatment group (Fig. 7D, F).

Cytofluorometric Analysis

Flow cytometry did not show a significant increase in endothelial progenitor cells in peripheral blood of rats undergone the 14-day ES treatment protocol (Fig. 8). However, an interesting subpopulation gating in the high right side of the scattergram could be detected (Fig. 8B). This cell population was CD45 negative and featured large dimensions and markedly increased cytoplasmic density. These findings were comparable with our previously published data on cytofluorometric analysis of in vitro electrostimulated cells.

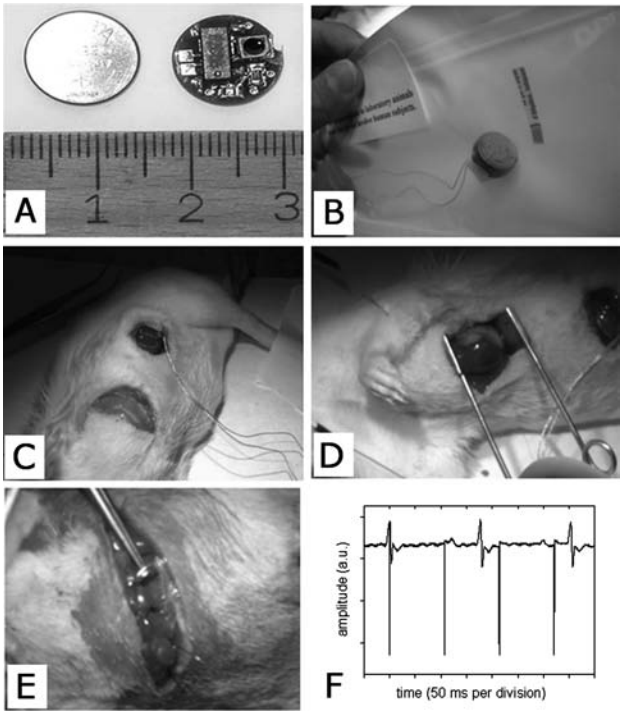

Figure 1. Experimental settings. (A, B) Electrostimulator. (C) Abdominal implant of microelectrostimulator. (D) Coronary ligation and induction of myocardial infarction. (E) Intraoperative image showing electrode tunnelized from the abdominal cavity to the thorax. (F) Graphic of registered electrical activity during stimulation. Spikes indicating stimuli delivery are not synchronous with the heart-derived ventricular complexes, indicating nonpacing conditions.

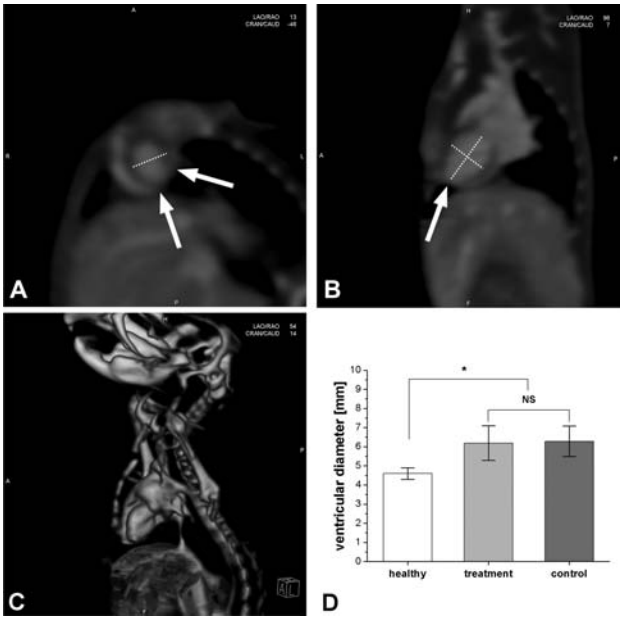

Figure 2. Myocardial infarction assessment and model validation by means of computed tomography (CT). (A, B) Representative images of myocardial infarction in a nonelectrostimulated (control) rat to show the methodology used. Left ventricular short-axis (A) and long-axis (B) reconstructions were acquired to evaluate status of myocardial tissue and to obtain accurate measurements of ventricular cavity. Arrows indicate the area of infarction, located in the left ventricular lateral wall. (C) 3D volume rendering reconstruction delineates the left ventricular apical pseudoaneurysm. (D) Bar chart of ventricular diameters in rats prior and following myocardial infarction. Data are presented as mean ± SD. Significant difference was found between the ventricular diameter measured in healthy and infarcted hearts ($p = 0.03$), while no significant difference was found between electrostimulated (ES) (treatment) and nonelectrostimulated (control) groups. (*) Significance at the 0.05 level; NS, nonsignificance.

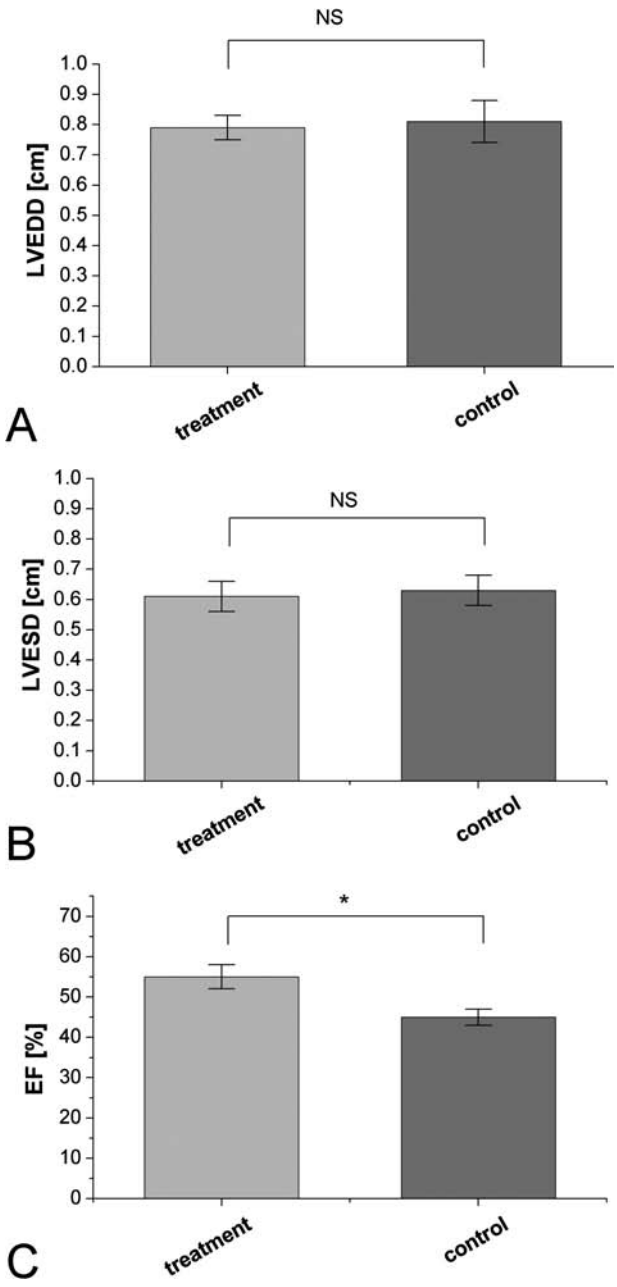

Figure 3. Morphometric and functional parameters in treatment and control groups. (A, B) Left ventricular end diastolic (A) and end systolic (B) diameters (LVEDD, LVESD) as calculated by angioCT. (C) Ejection fraction (EF) calculated by echocardiography. Data are presented as mean ± SD. *Significance at the 0.05 level; NS, nonsignificance.

DISCUSSION

Left ventricular remodeling is associated with myocyte apoptosis and cell replacement by fibrous tissue in the ventricular wall. This mechanism is considered to be the cause of cardiac dysfunction after an acute myocardial infarction. At the cellular level, sudden suppression of the oxygen supply triggers intricate molecular cascades, which modulate a series of critical biological events (17). Immediately following a myocardial infarction, the process of wound healing begins with the active migration of inflammatory cells, recruitment of cardiac fibroblasts, and eventual remodeling of the extracellular matrix to stabilize the infracted area and preserve ventricular wall function. However, cardiac function is seldom restored to normal. Cardiomyocyte loss and replacement by fibrous elements can result in progressive left ventricular remodeling and, eventually, congestive heart failure, a major public health problem (12).

Stem cell-based therapeutic strategies to restore myocardial cellularity and regenerate contractile tissue have generated considerable interest due to encouraging preliminary results (13,18,26,28). However, the answers to many questions concerning the ultimate fate and precise functional integration of injected stem cells remain unknown (34). Functional engraftment is required to augment synchronized contractility and avoid potentially life-threatening alterations in the electrical conduction of the heart (10,31). To address these issues, we have developed a cytokine-free system using cell ES as a novel means of inducing precommitment or conversion of fibroblasts to a myocardial phenotype. We previously demonstrated induction of cardiomyocyte precommitment in two fibroblast cell lines with different evolutive potential (8). This phenomenon, occurring in a stem cell phenotype as well (7), resulted in the expression of structural cardiac-specific proteins associated with the contractile apparatus and, importantly, with the proteins of the gap junctions integral to electromechanical coupling of cardiomyocytes in the heart, potentially leading to better cell functional integration. Our previous studies have also included the effects of long-term ES on human mesenchymal stem cells (hMSCs). ES-induced both morphological and biochemical changes in hMSCs, resulting in a shift toward a striated muscle cell phenotype expressing cardiac specific markers. This partially differentiated phenotype might allow a gradual, ongoing differentiation within the cardiac environment, providing time for both myocardial regeneration and electromechanical integration (7).

ES is widely used in rehabilitative medicine for its ability to restore muscle function reliably through induction of angiogenesis, promotion of cell proliferation, and inhibition of apoptosis (2,8,24). We sought to demonstrate increased angiogenesis and endothelial progenitor cell mobilization in an in vivo myocardial infarction ES model. We used a miniaturized multiparameter implantable stimulator to induce the ES of the infracted area. Parameters of ES were arranged in order to avoid a direct driving or pacing of native heart rhythm. Electrocardiographic recordings during pacing confirmed a nondriving activity on heart rhythm of the delivered electrical stimuli. The

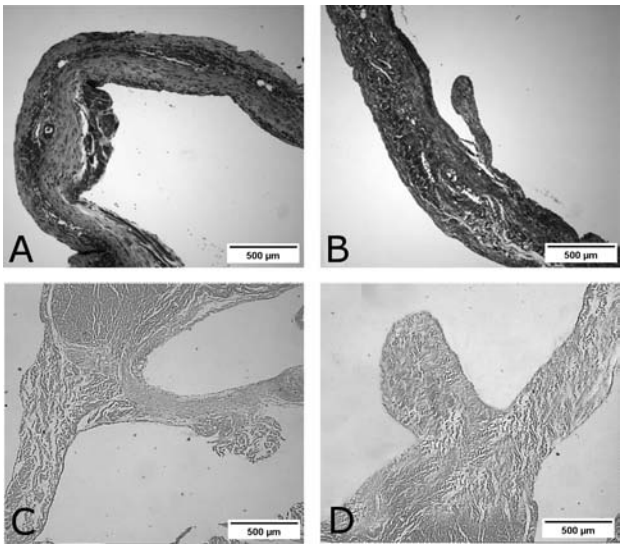

Figure 4. (A, B) Masson's trichrome staining of control non-ES hearts (A) and treatment ES hearts (B) to define and characterize the infarcted area (original magnification: 10×). (C, D) Representative H&E stainings of control (C) and treatment (D) groups (original magnification: 10×). Sections have been obtained at the level of anterolateral papillary muscle.

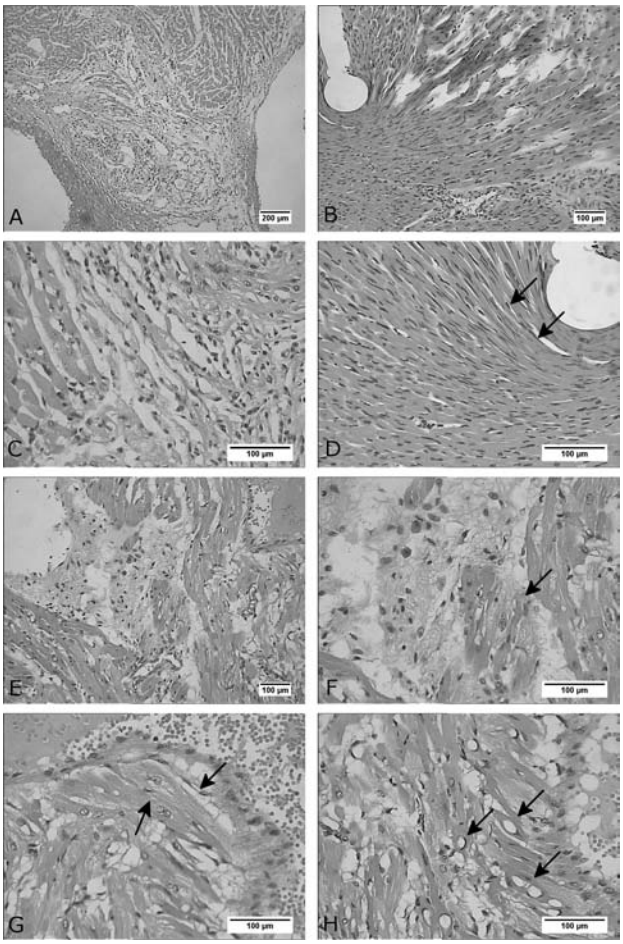

Figure 5. Histological evaluation of control hearts (A) and ES-treated hearts (B–H). (B) Electrode implantation site. Eosinophilic elongated spindle-shaped cells arranged in oriented manner were observed in proximity to the site of the electrode implant. Cells demonstrated an eccentric nucleus (arrows in D) and a fine cytoplasmic granularity (arrow in F). Other cells showed a fibrillar-like structure (arrows in G). Vascular structures were also present in the treatment group (arrows in H).

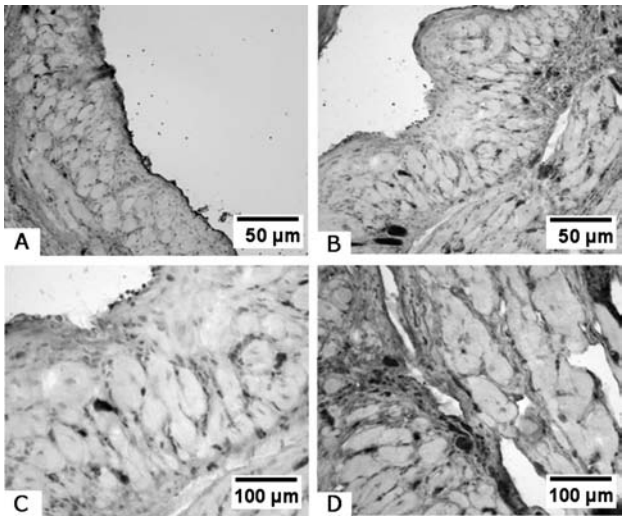

Figure 6. Immunohistochemistry for CD34. (A) Control group (original magnification: 20×). (B) Treatment group (original magnification: 20×). (C, D) Treatment group (original magnification: 40×). Enhanced presence of CD34-positive cells could be observed in the treatment group.

basis of this approach was the observation that ES prevents immobilization-induced muscle atrophy by minimizing (1) reduction of muscle fiber cross-sectional area, (2) interstitial fibrosis, and (3) impairment of the blood supply, due to improvements in capillary density and the capillary/fiber ratio (24). Mimicking the physiological stimulation conditions provides the correct sequence of signals to maintain and improve muscle structure and function. For this reason, we hypothesized that electrical stimuli could result in a biological shift of adult cells toward the muscle phenotype (14). ES of the cardiac cell environment mimics the electrical features of a beating heart and may direct the cellular apparatus of resident cells toward a cardiomyocyte configuration.

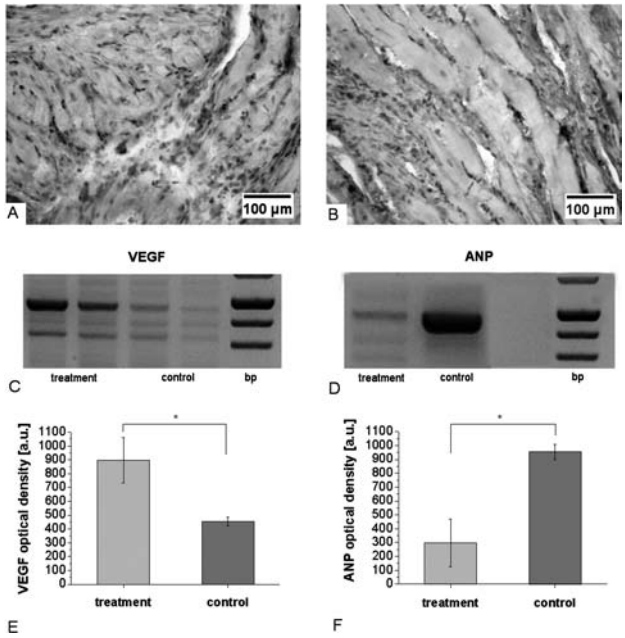

Figure 7. (A, B) Immunohistochemistry for VEGF. (A) Control group (original magnification: 40×). (B) Treatment group (original magnification: 40×). (C, D) RT-PCR and densitometry analysis for vascular endothelial growth factor (VEGF) (C) and atrial natriuretic peptide (ANP) (D). *Significance at the 0.05 level.

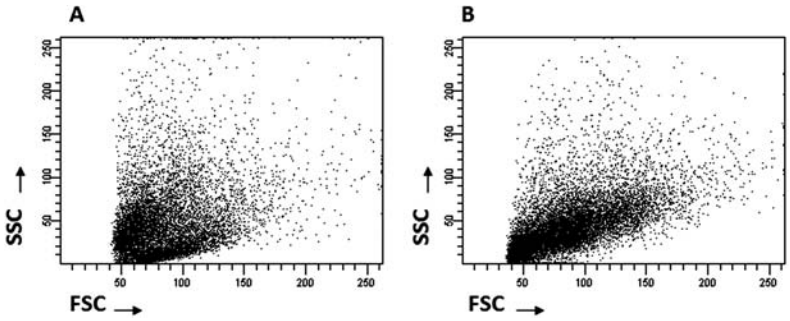

Figure 8. Flow cytometry analysis. Representative dot plots in control (A) and in treatment (B) groups. Note a subpopulation of elongated cells with high cytoplasmic density following electrostimulation.

In this study, we found changes at the cellular level in the myocardial scar zone, similar to those obtained with in vitro ES of fibroblasts. Cells within the infarcted zone and surrounding the electrode implant sites showed increased granularity and nuclear eccentricity, which are typical features of striated muscular cells. Considering the position of the nucleus, these cells presented characteristics of skeletal muscle fibers but were clearly located in a scar area, thus indicating a cell differentiating effect of in vivo ES. Along with these findings, the ejection fraction of treated animals significantly improved, without a significant modification in ventricular cavity diameters. In situ ES does not exert an effect on cardiac geometric remodeling but can positively affect tensile and elastomechanical properties of the myocardial scar, improving ventricle compliance and diastolic function. Considering this final effect, we can reliably speculate that the cytologic modifications of the fibroblasts populating the scar, resulting in a shift toward a muscular phenotype, could be at the basis of the improvement on the diastolic function. Whether this finding is actually playing a definite role in the improvement of cardiac function after in situ ES should be clarified with further studies.

Interestingly, we observed the appearance of a new subpopulation of elongated CD45-negative cells with high cytoplasmic density following ES. These findings were comparable with our previously published data on cytofluorometric analysis of in vitro electrostimulated cells. This cell population might be at the root of a proangiogenic drive, improving the microenvironment of the scar and overall cardiac function.

Immunohistology demonstrated an enhanced presence of CD34-positive cells in the myocardial infarct zone following ES, while quantitative analysis of CD34-positive cells in the peripheral blood failed to show a significant increase of mobilized progenitors. An explanation for these findings may be the migration and successive marginalization of the cells into the myocardium, according to the reported kinetics of progenitor cells migration in rats (4). This hypothesis is substantiated by the finding of increased levels of VEGF at 14 days following myocardial infarction. This finding was confirmed and quantified by RT-PCR, which demonstrated an increased expression of VEGF-related mRNA. Taken together, these findings indicate a proangiogenic drive induced by ES, which is confirmed by the presence of neovascular structures on histopathological evaluation.

However, authors acknowledge that data are not sufficient to fully ascertain whether they represent cells arising from bone marrow in response to ischemic injury or a resident population directly migrating from the surrounding myocardium to aid tissue repair.

Further studies could be useful to elucidate the origin of EPCs and the mechanism of action of ES concerning the neoangiogenetic drive. These investigations might include analysis of chemokines and chemoattractants involved in EPC homing at the injury site.

RT-PCR analysis also showed a decreased expression of ANP in the ES group when compared with control nonelectrostimulated infarcted hearts. ANP is a marker of cardiac heart failure whose production is stimulated by atrial distension subsequent to heart deterioration (15). In our study, ES reliably improved hemodynamic conditions manifest as a decrease in end diastolic pressures and atrial distension. Recently, Mukherjee et al. have performed long-term localized high-frequency electric stimulation within the myocardial infarct in pigs using a single lead pacemaker configuration (20). Although differences in experimental model, settings, and modalities of electrostimulation make the results obtained by these authors difficult to compare with the present work, the study provides intriguing data on the influence of ES on left ventricular wall thickness and remodeling of infarcted region as a result of a reduction in the regional metalloproteinases activity. The focus of our study has been put on the possible poststimulation regenerative drive induced by ES and confirmed by angiogenesis phenomena together with improved cardiac function. Even if we failed to demonstrate a significant positive remodeling of ventricular cavities, the reported decrease of ANP levels

testified a general improvement in hemodynamics that might contribute to the improvement in cardiac function.

In conclusion, our results concur to demonstrate a positive influence of ES on infarcted myocardium. These results extend our previous findings of in vitro progenitor cells electrostimulation and envision a potential application of this technology for regenerative purposes.

ACKNOWLEDGMENT: The authors declare no conflicts of interest.

REFERENCES

1. Behari, J. Changes in bone histology due to capacitive electric field stimulation of ovariectomized rat. Indian J. Med. Res. 130(6):720–725; 2009.
2. Carraro, U.; Rossini, K.; Mayr, W.; Kern, H. Muscle fiber regeneration in human permanent lower motoneuron denervation: Relevance to safety and effectiveness of FES-training, which induces muscle recovery in SCI subjects. Artif. Organs 29(3):187–191; 2005.
3. Chachques, J. C.; Mitz, V.; Hero, M.; Arhan, P.; Gallix, P.; Fontaliran, F.; Vilain, R. Experimental cardioplasty using the latissimus dorsi muscle flap. J. Cardiovasc. Surg. 26(5):457–462; 1985.
4. Delgaudine, M.; Lambermont, B.; Lancellotti, P.; Roelants, V.; Walrand, S.; Vanoverschelde, J. L.; Pierard, L.; Gothot, A.; Beguin, Y. Effects of granulocyte-colony-stimulating factor on progenitor cell mobilization and heart perfusion and function in normal mice. Cytotherapy 13(2):237–247; 2011.
5. DePace, D. M.; Webber, R. H. Electrostimulation and morphologic study of the nerves to the bone marrow of the albino rat. Acta Anat. 93(1):1–18; 1975.
6. Eberhardt, A.; Szczypiorski, P.; Korytowski, G. Effect of transcutaneous electrostimulation on the cell composition of skin exudate. Acta Physiol. Pol. 37(1):41–46; 1986.
7. Genovese, J. A.; Spadaccio, C.; Chachques, E.; Schussler, O.; Carpentier, A.; Chachques, J. C.; Patel, A. N. Cardiac pre-differentiation of human mesenchymal stem cells by electrostimulation. Front. Biosci. 14:2996–3002; 2009.
8. Genovese, J. A.; Spadaccio, C.; Langer, J.; Habe, J.; Jackson, J.; Patel, A. N. Electrostimulation induces cardiomyocyte predifferentiation of fibroblasts. Biochem. Biophys. Res. Commun. 370(3):450–455; 2008.
9. Genovese, J. A.; Spadaccio, C.; Rivello, H. G.; Toyoda, Y.; Patel, A. N. Electrostimulated bone marrow human mesenchymal stem cells produce follistatin. Cytotherapy 11(4):448–456; 2009.
10. Hagege, A. A.; Marolleau, J. P.; Vilquin, J. T.; Alheritiere, A.; Peyrard, S.; Duboc, D.; Abergel, E.; Messas, E.; Mousseaux, E.; Schwartz, K.; Desnos, M.; Menasché, P. Skeletal myoblast transplantation in ischemic heart failure: Long-term follow-up of the first phase I cohort of patients. Circulation 114(1 Suppl):I108–I113; 2006.
11. Hulmes, H. Kelley's Textbook of Internal Medicine, 4th ed. MD: Lippincott, Williams and Wilkins; 2000.
12. Itescu, S.; Schuster, M. D.; Kocher, A. A. New directions in strategies using cell therapy for heart disease. J. Mol. Med. 81(5):288–296; 2003.
13. Jolicoeur, E. M.; Granger, C. B.; Fakunding, J. L.; Mockrin, S. C.; Grant, S. M.; Ellis, S. G.; Weisel, R. D.; Goodell, M. A. Bringing cardiovascular cell-based therapy to clinical application: Perspectives based on a National Heart, Lung, and Blood Institute Cell Therapy Working Group meeting. Am. Heart J. 153(5):732–742; 2007.
14. Kawahara, Y.; Yamaoka, K.; Iwata, M.; Fujimura, M.; Kajiume, T.; Magaki, T.; Takeda, M.; Ide, T.; Kataoka, K.; Asashima, M.; Yuge, L. Novel electrical stimulation sets the cultured myoblast contractile function to 'on'. Pathobiology 73(6):288–294; 2006.
15. Kimura, K.; Yamaguchi, Y.; Horii, M.; Kawata, H.; Yamamoto, H.; Uemura, S.; Saito, Y. ANP is cleared much faster than BNP in patients with congestive heart failure. Eur. J. Clin. Pharmacol. 63(7):699–702; 2007.
16. Kuramochi, Y.; Guo, X.; Sawyer, D. B.; Lim, C. C. Rapid electrical stimulation induces early activation of kinase signal transduction pathways and apoptosis in adult rat ventricular myocytes. Exp. Physiol. 91(4):773–780; 2006.
17. Leferovich, J. M.; Bedelbaeva, K.; Samulewicz, S.; Zhang, X. M.; Zwas, D.; Lankford, E. B.; Heber-Katz, E. Heart regeneration in adult MRL mice. Proc. Natl. Acad. Sci. USA 98(17):9830–9835; 2001.
18. Mazo, M.; Gavira, J. J.; Abizanda, G.; Moreno, C.; Ecay, M.; Soriano, M.; Aranda, P.; Collantes, M.; Alegria, E.; Merino, J.; Peñuelas, I.; García Verdugo, J. M.; Pelacho, B.; Prósper, F. Transplantation of mesenchymal stem cells exerts a greater long-term effect than bone marrow mononuclear cells in a chronic myocardial infarction model in rat. Cell Transplant. 19(3):313–328; 2010.
19. Modlin, M.; Forstner, C.; Hofer, C.; Mayr, W.; Richter, W.; Carraro, U.; Protasi, F.; Kern, H. Electrical stimulation of denervated muscles: First results of a clinical study. Artif. Organs 29(3):203–206; 2005.
20. Mukherjee, R.; Rivers, W. T.; Ruddy, J. M.; Matthews, R. G.; Koval, C. N.; Plyler, R. A.; Chang, E. I.; Patel, R. K.; Kern, C. B.; Stroud, R. E.; Spinale, F. G. Long-term localized high-frequency electric stimulation within the myocardial infarct: Effects on matrix metalloproteinases and regional remodeling. Circulation 122(1):20–32; 2010.
21. Naumann, K.; Pette, D. Effects of chronic stimulation with different impulse patterns on the expression of myosin isoforms in rat myotube cultures. Differentiation 55(3):203–211; 1994.
22. Oshima, H.; Payne, T. R.; Urish, K. L.; Sakai, T.; Ling, Y.; Gharaibeh, B.; Tobita, K.; Keller, B. B.; Cummins, J. H.; Huard, J. Differential myocardial infarct repair with muscle stem cells compared to myoblasts. Mol. Ther. 12(6):1130–1141; 2005.
23. Parreno, M.; Pol, A.; Cadefau, J.; Parra, J.; Alvarez, L.; Membrilla, E.; Cusso, R. Changes of skeletal muscle proteases activities during a chronic low-frequency stimulation period. Pflugers Arch. 442(5):745–751; 2001.
24. Qin, L.; Appell, H. J.; Chan, K. M.; Maffulli, N. Electrical stimulation prevents immobilization atrophy in skeletal muscle of rabbits. Arch. Phys. Med. Rehabil. 78(5):512–517; 1997.
25. Russold, M.; Jarvis, J. C. Implantable stimulator featuring multiple programs, adjustable stimulation amplitude and bi-directional communication for implantation in mice. Med. Biol. Eng. Comput. 45(7):695–699; 2007.
26. Sant'anna, R. T.; Kalil, R. A.; Pretto Neto, A. S.; Pivatto Junior, F.; Fracasso, J.; Sant'anna, J. R.; Marques, M.; Markoski, M.; Prates, P. R.; Nardi, N. B.; Nesralla, I. A. Global contractility increment in nonischemic dilated cardiomyopathy after free wall-only intramyocardial

injection of autologous bone marrow mononuclear cells: An insight over stem cells clinical mechanism of action. Cell Transplant. 19(8):959–964; 2010.
27. Scheubel, R. J.; Zorn, H.; Silber, R. E.; Kuss, O.; Morawietz, H.; Holtz, J.; Simm, A. Age-dependent depression in circulating endothelial progenitor cells in patients undergoing coronary artery bypass grafting. J. Am. Coll. Cardiol. 42(12):2073–2080; 2003.
28. Segers, V. F.; Lee, R. T. Stem-cell therapy for cardiac disease. Nature 451(7181):937–942; 2008.
29. Shafy, A.; Lavergne, T.; Latremouille, C.; Cortes-Morichetti, M.; Carpentier, A.; Chachques, J. C. Association of electrostimulation with cell transplantation in ischemic heart disease. J. Thorac. Cardiovasc. Surg. 138(4):994–1001; 2009.
30. Simon, A. J.; Casimiro, D. R.; Finnefrock, A. C.; Davies, M. E.; Tang, A.; Chen, M.; Chastain, M.; Kath, G. S.; Chen, L.; Shiver, J. W. Enhanced in vivo transgene expression and immunogenicity from plasmid vectors following electrostimulation in rodents and primates. Vaccine 26(40):5202–5209; 2008.
31. Smits, P. C. Myocardial repair with autologous skeletal myoblasts: A review of the clinical studies and problems. Minerva Cardioangiol. 52(6):525–535; 2004.
32. Takuma, S.; Suehiro, K.; Cardinale, C.; Hozumi, T.; Yano, H.; Shimizu, J.; Mullis-Jansson, S.; Sciacca, R.; Wang, J.; Burkhoff, D.; Di Tullio, M. R.; Homma, S. Anesthetic inhibition in ischemic and nonischemic murine heart: Comparison with conscious echocardiographic approach. Am. J. Physiol. Heart Circ. Physiol. 280(5):H2364–H2370; 2001.
33. Viscor, G.; Javierre, C.; Pages, T.; Ventura, J. L.; Ricart, A.; Martin-Henao, G.; Azqueta, C.; Segura, R. Combined intermittent hypoxia and surface muscle electrostimulation as a method to increase peripheral blood progenitor cell concentration. J. Transl. Med. 7:91; 2009.
34. Westrich, J.; Yaeger, P.; He, C.; Stewart, J.; Chen, R.; Seleznik, G.; Larson, S.; Wentworth, B.; O'Callaghan, M.; Wadsworth, S.; Akita, G.; Molnar, G. Factors affecting residence time of mesenchymal stromal cells (MSC) injected into the myocardium. Cell Transplant. 19(8):937–948; 2010.